

# What is the physics behind the ${}^3\text{He}$ – ${}^4\text{He}$ anomaly?

 W. Neubert<sup>1</sup>, A.S. Botvina<sup>2,3</sup>
<sup>1</sup> Institut für Kern- und Hadronenphysik, Forschungszentrum Rossendorf, 01314 Dresden, Germany

<sup>2</sup> Istituto Nazionale di Fisica Nucleare, 40126 Bologna, Italy

<sup>3</sup> Institute for Nuclear Research, Russian Academy of Science, 117312 Moscow, Russia

Received: 24 September 1999 / Revised version: 22 November 1999

Communicated by B. Povh

**Abstract.** We show that coalescence of nucleons emitted prior to thermalization in highly excited nuclei can explain the anomaly of kinetic energies of helium clusters. A new coalescence algorithm has been included in the statistical approach to nuclear reactions formerly used to describe intermediate mass fragment production.

**PACS.** 25.70.-z Low and intermediate energy heavy-ion reactions – 25.70.Pq Multifragment emission and correlations

## 1 Introduction

In this paper we address a phenomenon which seems to be important for understanding mechanisms which favour light cluster production in intermediate energy reactions. It concerns the so-called  ${}^3\text{He}$ – ${}^4\text{He}$  “puzzle”, i.e. the anomalous behaviour of their kinetic energies. Usually, thermal models (e.g. [1]) or approaches which consider a possible radial expansion (flow) [2] are applied to describe the kinetic energies of light charged particles (LCP). In the thermal scenario we expect  $\langle E_{kin}({}^3\text{He}) \rangle \approx \langle E_{kin}({}^4\text{He}) \rangle$  whereas radial flow delivers  $\langle E_{kin}({}^3\text{He}) \rangle < \langle E_{kin}({}^4\text{He}) \rangle$ . However, in many reactions quite an opposite behaviour has been observed. The corresponding data are summarized in Table 1. For example, there is evidence of the “puzzle” in the inclusive kinetic energy spectra of He isotopes obtained from p + Ag [3] and p+C [4] reactions at 1 GeV, in 7.5 GeV/c proton collisions with  ${}^{12}\text{C}$ ,  ${}^{112,124}\text{Sn}$ ,  ${}^{197}\text{Au}$  [5] and in Ne+U reactions at 250 and 400 A·MeV [6]. The anomaly was also observed in antiproton reactions 202 MeV/c  $\bar{p}$  +  ${}^{12}\text{C}$ ,  ${}^{40}\text{Ca}$ ,  ${}^{63}\text{Cu}$ ,  ${}^{92,98}\text{Mo}$  and  ${}^{238}\text{U}$  [7]. Precise measurements of 55 MeV  ${}^3\text{He}$ +Ag collisions at  $\Theta_{lab}=147.5^\circ$  also have shown the anomalous behaviour of  ${}^3\text{He}$  and  ${}^4\text{He}$  ([8]). The following trends have been observed in heavy-ion collisions: (i) the difference  $\Delta E = \langle E_{kin}({}^3\text{He}) \rangle - \langle E_{kin}({}^4\text{He}) \rangle$  is positive and increases with the particle multiplicity in Au + Au reactions at 250 A·MeV [9], (ii) the “puzzle” is pronounced in central event samples of Au + Au [10], 95 A·MeV Ar + Ni [11], 50 A·MeV Xe+Sn [12] but weaker in Ar + Ca [13] collisions, (iii) positive values  $\Delta E$  are observed in the incident energy range from about 50 A·MeV to 300 A·MeV but the anomaly vanishes at  $\simeq 1$  GeV [14]. The existing data indicate that the larger the number of nucleons of the colliding

system the larger the deviation of the kinetic energies of  ${}^3\text{He}$  and  ${}^4\text{He}$ .

An appropriate way to describe processes involving many particles is the statistical approach. The system characterized in the initial stage by nonequilibrium distribution functions evolves towards equilibration as a result of interaction between particles. In this process the system runs through different states. The first one can be considered as equilibration of the one-particle degrees of freedom. In the following the evolution toward total thermalization can be considered as progressive involving of higher order particle correlations. For finite expanding systems one cannot predict in advance what kind of equilibration should be considered.

It is usually accepted that Intermediate Mass Fragments (IMF) observed in multifragmentation processes are mainly produced in a state close to thermalization. This assumption is supported by the success of statistical multifragmentation models, e.g. SMM [15] and MMMC [16]. However, this conclusion may not be true for composite particles like  ${}^3\text{He}$  and  ${}^4\text{He}$  which can be formed in earlier stages of the reaction. We guess that their unexpected behaviour results from an interplay of different production mechanisms.

## 2 Production of composite particles by coalescence

First we point at an alternative way to form clusters. We start from a distribution of nucleons in the phase space at some “freeze-out” time obtained after a dynamical evolution. Generally, non-uniform distributions are conceivable.

**Table 1.** Experimental data concerning the  ${}^3\text{He}$ - ${}^4\text{He}$  anomaly. The temperatures  $T$  of the helium isotopes were obtained by Maxwell-Boltzmann fits to the kinetic energy distributions, in case of \*) an exponential fit to the data at  $\Theta_{lab}=90^\circ$  was applied

Reaction	Incident energy or momentum	$T({}^3\text{He})$ (MeV)	$T({}^4\text{He})$ (MeV)
p+ ${}^{12}\text{C}$ [4]	1 GeV	6.8±0.2	5.8±0.2
p+Ag [3]	1 GeV	11.2±0.2	4.6±0.1
$\bar{p}$ + ${}^{12}\text{C}$ [7]	202 MeV/c	19.8±12.	15.6±9.
$\bar{p}$ + ${}^{40}\text{Ca}$ [7]	202 MeV/c	24.2±13.	16.8±9
$\bar{p}$ + ${}^{63}\text{Cu}$ [7]	202 MeV/c	22.2±10.	15.4±8.
$\bar{p}$ + ${}^{92}\text{Mo}$ [7]	202 MeV/c	25.2±17.	16.2±9.
$\bar{p}$ + ${}^{98}\text{Mo}$ [7]	202 MeV/c	21.8±6.	17.1±7.
$\bar{p}$ + ${}^{238}\text{U}$ [7]	202 MeV/c	20.1±12.	14.2±4.
p+ ${}^{12}\text{C}$ [5]	7.5 GeV/c	37.±2.	28.±2.
p+ ${}^{112}\text{Sn}$ [5]	7.5 GeV/c	38.±1.	27.±1.
p+ ${}^{124}\text{Sn}$ [5]	7.5 GeV/c	43.±1.	27.±1.
p+Au [5]	7.5 GeV/c	50.±2.	33.±2.
${}^{20}\text{Ne}$ +U [6]	250 A·MeV	36.6±0.3*	31.9±4.2*
${}^{20}\text{Ne}$ +U [6]	400 A·MeV	46.5±1.3*	37.3±3.3*
		$\langle E_{kin}({}^3\text{He}) \rangle$ (MeV)	$\langle E_{kin}({}^4\text{He}) \rangle$ (MeV)
p+Ag [3]	1 GeV	17.7±0.3	12.7±0.2
${}^3\text{He}$ +Ag [8]	55 MeV	19.8	15.6
Ar+ Ni [11]	50-100 A·MeV	32.5	26.2
Xe+Sn [12]	50 A·MeV	51.0	33.0
Ar+Xe [13]	400 A·MeV	139.6±2.5	134.0±6.1
Au+Au [10]	100 A·MeV	85.0±4.0	59.0±2.0
Au+Au [10]	150 A·MeV	101.0±4.0	77.0±5.0
Au+Au [10]	250 A·MeV	147.0±4.0	136.0±3.0

But in some experiments, e.g. central nucleus–nucleus collisions [17], it is possible to select events which are nearly isotropic in space and look like thermal ones. Therefore, in such cases, we can simply assume that the nucleons populate the available *many-body* phase space uniformly, i.e. there is equilibration in one-particle degrees of freedom, that gives rise to a thermal distribution for individual nucleons in thermodynamical limit.

A composite particle can be formed from two or more nucleons if they are close to each other in the phase space. This simple prescription is known as coalescence model and it reflects the properties of the nucleon–nucleon interaction. Here we use the coalescence in momentum space only. The basic assumption is that the dynamical process which leads to a momentum redistribution is very fast (nearly instantaneous) so that the coordinates of nucleons are just defined by their momenta. It is also justified taking into account quantum properties of the system since the wave functions of nucleons are rather broad. This type of coalescence model has proven successful in reproducing experimental data (see e.g. [18–20]).

In the standard formulation of the model it is assumed that the fragment density in momentum space is proportional to the nucleon density times the probability of finding nucleons within a small sphere of the coalescence ra-

dius  $p_0$ . From this hypothesis an *analytical* expression can be derived for differential yields of coalescent clusters [18, 20]:

$$\left( E_A \frac{d^3 N_A}{d\bar{p}_A^3} \right) = \frac{2S_A + 1}{2^A} \frac{1}{\nu!} \frac{1}{z!} \left( \frac{4\pi}{3} \frac{p_0^3}{m_n} \right)^{A-1} \left( E_n \frac{d^3 N_n}{d^3 \bar{p}_n} \right)^A$$

where  $E_A, E_n, \bar{p}_A$  and  $\bar{p}_n$  are the energies and the momenta of fragments and nucleons,  $\nu$  and  $z$  are the numbers of neutrons and protons ( $A = \nu + z$ );  $S_A$  is the spin of the fragment with mass number  $A$  and  $m_n \approx 0.94$  GeV is the nucleon mass. However, this equation disregards correlations between different clusters since the conservation of the nucleon number is not taken into account. Therefore, the above formulae is valid only for  $N_{A=1} \gg N_{A=2} \gg N_{A=3} \dots$ . In many reactions this condition is not fulfilled.

We developed an alternative formulation of the coalescence model which is suitable for computer simulations. Nucleons can produce a cluster with mass number  $A$  if their momenta relative to the center-of-mass moment of the cluster is less than  $p_0$ . Accordingly we take  $|\mathbf{p}_i - \mathbf{p}_{cm}| < p_0$  for all  $i = 1, \dots, A$ , where  $\mathbf{p}_{cm} = \frac{1}{A} \sum_{i=1}^A \mathbf{p}_i$ . This is performed by comparing the momenta of all nucleons. In the following examples the value  $p_0 \approx 94$  MeV/c has been adopted corresponding to relative velocities  $v_{rel}=0.1c$  in agreement with previous analyses [19].

We note a problem which is sometimes disregarded in these simulations. Some nucleons may have such momenta that they can belong to different coalescent clusters according to the coalescence criterion. In these cases the final decision depends on the sequence of nucleons within the algorithm. To avoid this uncertainty we developed an iterative coalescence procedure.  $M$  steps are calculated in the coalescence routine with the radius  $p_{0j}$  which is increased at each step  $j$ :  $p_{0j} = (j/M) \cdot p_0$  ( $j = 1, \dots, M$ ). Clusters produced at earlier steps participate as a whole in the following steps. In this case the final clusters not only meet the coalescence criterion but also the nucleons have the minimum distance in the momentum space. Mathematically exact, this procedure gives correct results in the limit  $M \rightarrow \infty$  but we found that in practical calculations it is sufficient to confine the steps to  $M=5$ .

To demonstrate how fragments are produced by coalescence we take as an example a nuclear system with mass number  $A_0 = 200$  and charge  $Z_0 = 80$  at various excitation energies  $E^*=10, 20, 30$  and 100 A·MeV. We disintegrate the system into nucleons by taking away about 7 A·MeV (binding energy). The rest of the energy turns into the kinetic energies of nucleons which populate the whole available many-body momentum phase space uniformly. We use the procedure developed in [21] to generate momenta. Example mass distributions of generated fragments are shown in Fig. 1. At low excitation energies we see one big “coalescent” cluster and some light fragments (an “U–shape” distribution). With increasing excitation energy the large cluster will be destroyed and several small clusters are produced. At about 30 A·MeV a transition appears which changes the mass distribution into a “step”-like one. At higher energies an exponential-like shape of the mass distribution occurs and that corresponds to the

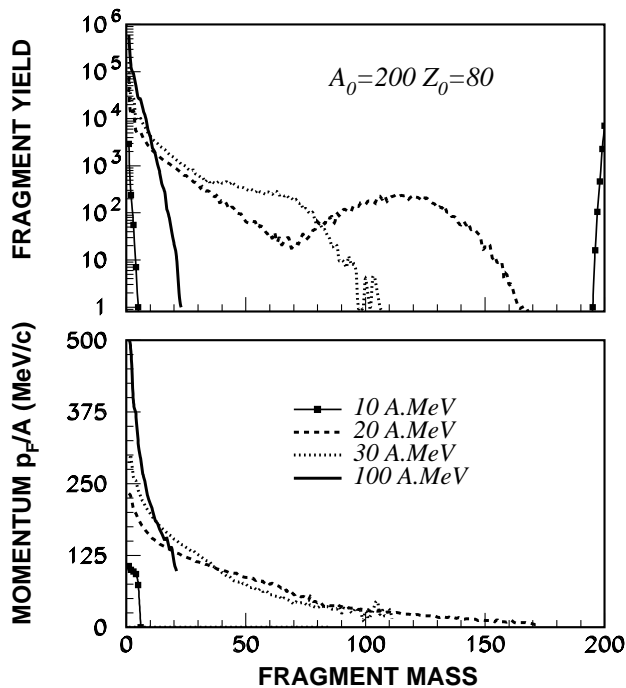


**Fig. 1.** Fragment production by coalescence. Upper panel: fragment yields per  $10^4$  generated events at 4 different excitation energies. Lower panel: the corresponding fragment momenta per nucleon

standard coalescence picture at high energies. We found that this transition happens at  $\langle p \rangle / p_0 \approx 2$ , where  $\langle p \rangle$  is the average momentum of thermalized nucleons, and it depends weakly on the size and other parameters of the system. In Fig. 1 we show also the average momenta of the clusters. We see that the coalescence provides a special ordering in the kinetic energy of the fragments: light clusters have larger energies per nucleon than the heavy ones. Large clusters are preferentially formed from nucleons with small momenta, i.e. which are closer to the center of the phase space.

The evolution of the mass distribution with excitation energy predicted by the coalescence model corresponds to our expectations for the decay of finite nuclei. Large clusters must be excited if they are treated in the classical coalescence model because there is a motion of nucleons with respect to the center of mass of the clusters. In this case a big coalescent cluster can be treated as an excited remnant of the system in which more complete equilibration is achieved and which can decay in a thermal-like way. Such a picture is supported by dynamical calculations which show the different reaction stages in nucleus–nucleus collisions at higher energies (e.g. [22]). After the first interactions some nucleons immediately leave the system and we can assume that later on they form coalescent clusters in final state interactions. This fast emission lowers essentially the energy of the remaining part and favours its equilibration, so we have a chance to treat it by statistical methods.

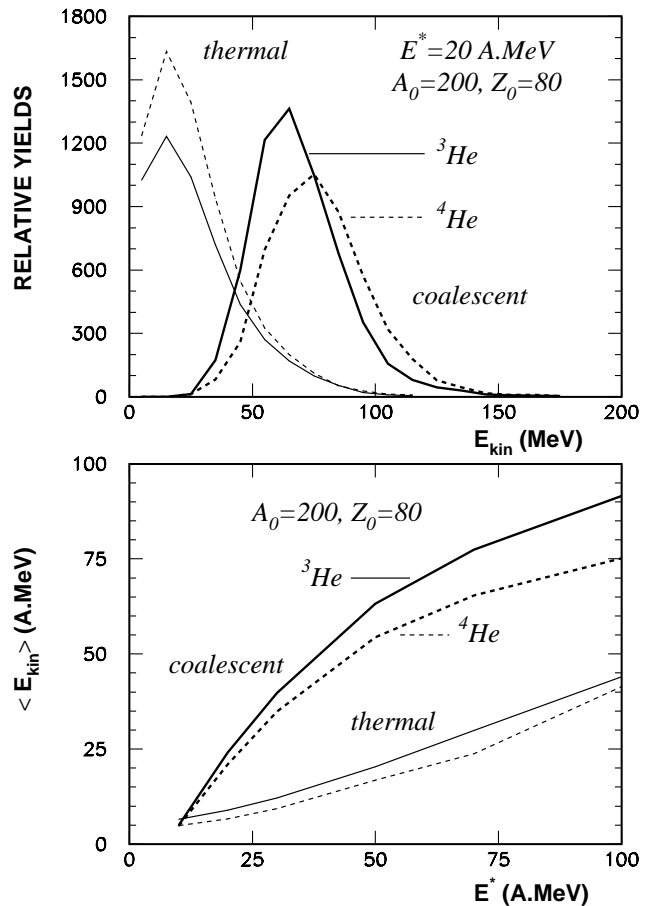


**Fig. 2.** Kinetic energy spectra (top) and mean kinetic energies per nucleon (versus excitation energy, bottom) of  ${}^3\text{He}$  and  ${}^4\text{He}$  calculated for the thermal and coalescence scenarios

### 3 Kinetic energies of ${}^3\text{He}$ and ${}^4\text{He}$

Now we show qualitatively how the coalescence can explain the “puzzle”. In Fig. 2 (top) we present the kinetic energy distributions of coalescent clusters  ${}^3\text{He}$  and  ${}^4\text{He}$  generated for  $E^* = 20 \text{ A.MeV}$ . The peaks in both spectra are shifted towards higher energies similar to collective motion (radial flow). For a different (e.g. non-equilibrium) initial distribution of the nucleons in momentum space we expect broader spectra with possible shifts of the peaks. But, in any case, the kinetic energies of the clusters will be high. In the bottom of Fig. 2 we plot the mean kinetic energies of helium isotopes for two scenarios and different excitation energies. The coalescent  ${}^3\text{He}$  clusters have slightly larger kinetic energy per nucleon compared with  ${}^4\text{He}$ . This energy difference increases with excitation energy though the total kinetic energy of  ${}^3\text{He}$  is still lower than the energy of  ${}^4\text{He}$ . This is caused by the mentioned correlation between the cluster production and the momenta of nucleons which form the clusters (Fig. 1, bottom). Such a correlation was already under discussion, e.g. [23], to explain the observed radial-flow energies of the fragments. In Fig. 2 we also show the kinetic energies and spectra of  ${}^3\text{He}$  and  ${}^4\text{He}$  calculated with the SMM

code [15] assuming a completely thermalized system at the same excitation energies. Herewith all thermal processes including deexcitation of hot primary fragments are taken into account. There is a striking difference in the kinetics of light clusters produced by coalescence or thermal mechanisms. In high energy reactions the difference may even increase because the energy released in the preequilibrium stage is usually much larger than the remaining equilibrium energy. We have checked also the influence of secondary deexcitations of possibly excited intermediate coalescent clusters (with  $A > 4$ ) on the spectra of the helium isotopes: the energy decrease is relatively small and the difference to the thermal spectra remains pronounced.

We expect that the thermal fragment production and the coalescence coexists in heavy-ion collisions over a wide energy range. The final shapes of the fragment spectra depend on their relative contributions. It is well known that the equilibrium decay provides a large number of  $\alpha$ -particles, whereas  ${}^3\text{He}$  clusters are suppressed. But  ${}^3\text{He}$  clusters can be produced predominantly by coalescence from the large number of emitted preequilibrium nucleons. As a result, the kinetic energies of  ${}^3\text{He}$  become larger compared with those of the  $\alpha$ -clusters. Such conditions may occur at intermediate energies in heavy ion reactions. However, in central nucleus-nucleus collisions the size of the thermalized source decreases with increasing beam energy as shown by SMM calculations and comparison with experimental data [24, 25]. Thus at sufficient high energies the coalescence becomes a dominant production mechanism for both kinds of He clusters and their kinetic energies may be very similar.

#### 4 Comparison of experimental data with SMM and coalescence calculations

We checked this hypothesis by calculations of fragment production in central  $Au + Au$  collisions using the SMM model which was modified by inclusion of radial flow and preequilibrium particle emission. Recently this approach was used in ref's. [22, 24–26]. In the framework of this model it is assumed that the total c.m. energy is shared between a thermal source (responsible for IMF and thermal LPC production), creation of pions (taken phenomenologically from experimental data) and preequilibrium emission of nucleons. Afterwards, these nucleons may coalesce into composite particles. A uniform initial distribution of “preequilibrium” nucleons in many-body momentum space is assumed. As already mentioned this assumption allows to estimate simply the influence of coalescence in the particular case of central events.

The excitation energy and mass of the equilibrium sources were parametrized by fitting the charge distributions and multiplicities of IMF's in the beam energy range from 150 to 1050 A·MeV as described in [24]. The radial flow was found by fitting the kinetic energy spectra of IMF's and it matches the experimental systematics [17, 27]. The source parameters at 1150 A·MeV [14] obtained by extrapolation are very close to that at 1050 A·MeV. In

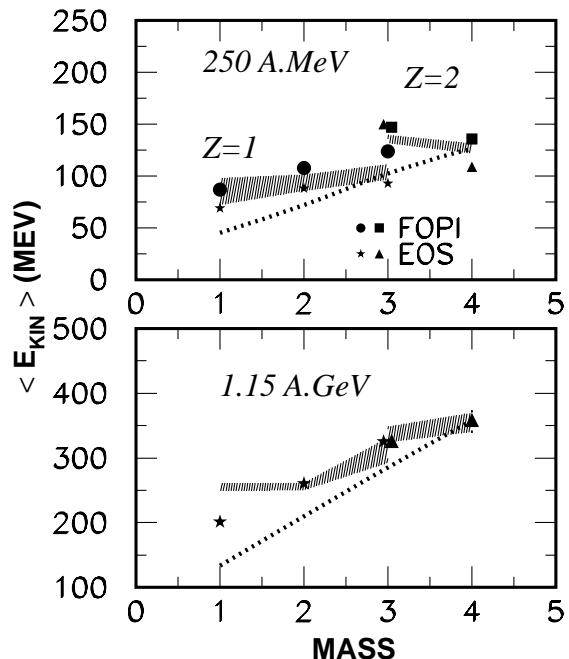


**Fig. 3.** Mean kinetic energies vs. mass number of LCP's in central collisions of Au on Au at incident energies 250 and 1150 A·MeV. Black symbols: data, dotted line: thermal production only, shadowed area: thermal origin and coalescence ( $v_{rel}=0.1c$ ) assuming an overall uncertainty of  $\simeq 15\%$  in the model parameters

[24, 25] it has been concluded that the size of the thermal source decreases considerably with the beam energy, and preequilibrium emission becomes important. The part of energy attributed to the preequilibrium stage is very large and, therefore, the masses of the coalescence fragments decrease nearly exponentially. In Fig. 3 we compare the experimental data from central Au+Au collisions with the calculated mean kinetic energies of light charged particles. The energy spectra of  ${}^3\text{He}$  and  ${}^4\text{He}$  were simulated for 250 A·MeV in the angular range  $60^\circ \leq \Theta_{cm} \leq 90^\circ$  using the lower and upper registration thresholds given in [10]. LCP's emitted from the thermal source with superimposed collective motion show the expected increase of  $\langle E_{kin} \rangle$  with  $A$ . However, the energy stored in preequilibrium nucleons is decisive for clusters predominantly produced from these nucleons: the  ${}^3\text{He}$ - ${}^4\text{He}$  anomaly appears if a substantial part of  ${}^3\text{He}$  comes from coalescence whereas the thermal production of  ${}^4\text{He}$  dominates. In addition we show in Table 2 a reasonable reproduction of the hydrogen and helium multiplicities within this scenario.

Enhanced production of  ${}^3\text{He}$  with increasing beam energy has been established in central Au+Au collisions [10, 28, 29] as shown in Fig. 4. The  ${}^3\text{He}$  yield dominates over  ${}^4\text{He}$  production in the region  $\geq 600$  A·MeV. Calculations with our model confirm this trend. There is an obvious surplus of  ${}^3\text{He}$  by coalescence with respect to the thermal production. This behaviour seems to be related to the disappearance of the anomaly established at 1.15 A·GeV [14],

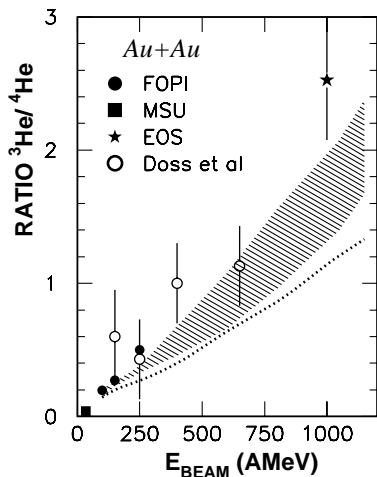


**Fig. 4.** Yield ratio  ${}^3\text{He}/{}^4\text{He}$  in central Au+Au collisions vs. beam energy. Symbols show the data, dotted line: equilibrium-source calculations with the parameter set from [24], shaded area: calculations including preequilibrium and coalescence, similar to Fig. 3

Fig. 3, that is also present in our calculations. The disagreement in the calculated proton energies may be caused by the centrality criterion in [14] which is different from that in [10]. Selection of protons around  $\Theta_{cm} \simeq 90^\circ$  in events with high multiplicity may push down their kinetic energies since such a criterion includes many events with predominantly forward-backward directed high energy nucleons. Indeed, lower proton energies were obtained by simulations assuming anisotropic preequilibrium emission of nucleons whereas the conclusion about the  ${}^3\text{He}$ - ${}^4\text{He}$  anomaly is maintained.

## 5 Conclusions

Summarizing we found that the appearance and disappearance of the  ${}^3\text{He}$ - ${}^4\text{He}$  anomaly reflects an interplay of equilibrium and nonequilibrium processes in these reactions. Besides the thermal emission the coalescence of nonequilibrium nucleons was found to be the important process which is responsible for enhanced mean kinetic energies of  ${}^3\text{He}$ . The effect is pronounced when both the thermal production and the coalescence contributions are comparable. At sufficient high energies only a small part of the colliding nuclei attains equilibration and both  ${}^4\text{He}$  and  ${}^3\text{He}$  are mainly produced by coalescence. As a consequence, the anomalous behaviour vanishes.

We mention another approach [12] which shows that in central nucleus-nucleus collisions around the Fermi energy a fast fragment emission during the expansion stage (described by the EES model [30]) can be responsible for the ‘‘puzzle’’. This explanation is qualitatively in agreement with our findings. However, we suppose that coalescence is a general mechanism which may be applied successfully in statistical or dynamical models (see e.g. [6, 31, 32]). It seems that the correlation between energies

**Table 2.** Multiplicities of LCP’s in central Au+Au collisions. Typical sum uncertainties of the calculations are  $\pm 5$

	E(A·MeV)	pre	equ	sum	data, [17]
Z=1	150	32.2	32.4	64.6	61.84(0.58)
Z=1	250	52.2	30.8	83.0	75.82(0.62)
Z=1	400	60.0	34.8	94.8	92.04(0.62)
Z=2	150	5.3	15.6	20.9	26.76(0.36)
Z=2	250	8.9	14.5	23.4	27.27(0.36)
Z=2	400	9.3	14.3	23.6	24.16(0.30)

and masses of the clusters predicted by the coalescence model may explain the observed features of fragment production in a wide energy range.

This work was supported by the German Ministry of Education and Research (BMBF) under contract 06-DR-828. A.S.B. thanks the INFN (Bologna section) for hospitality and support. We acknowledge stimulating discussions with H.-W.Barz and W.Reisdorf.

## References

1. A.Z.Mekjian, Phys. Rev. C **17**, 1051 (1978)
2. P.J.Siemens and J.O.Rasmussen, Phys. Rev. Lett. **42**, 880 (1979)
3. E.N.Volnin et al., LNPI Gatchina Nr.101,1974 (unpublished)
4. L.N.Andronenko et al., PNPI Gatchina NP-3-1998 / 2217-1998 (unpublished)
5. V.I.Bogatina et al., Yad. Fiz. **32**, 1363 (1980)
6. H.H.Gutbrod et al., Phys. Rev. Lett. **37**, 667 (1976)
7. W.Markiel et al., Nucl. Phys. A **485**, 445 (1988)
8. V.E.Viola, K.Kwiatkowski and W.A.Friedman, Indiana State University IUCF-40007-116, 1998 (unpublished)
9. K.G.R.Doss et al., Phys. Rev. Lett. **59**, 2720 (1987) and Mod. Phys. Lett. A **3**, 849 (1988)
10. G. Poggi et al., FOPI collaboration, Nucl. Phys. A **324**, 1777 (1993) and private communication
11. B.Borderie et al., in *Proceedings of the International Workshop on Heavy Ion Physics at Low, Intermediate and High Energies using 4 $\pi$  Detectors, Poiana Brasov, 1996* edited by M.Petrovici et al. (World Scientific, Singapore 1997) p.96
12. R.Bougault et al., in *Proceedings of the XXVII International Workshop on Gross Properties of Nuclei and Nuclear Excitations, Hirschegg, 1999* edited by H.Feldmeier (GSI Darmstadt, 1999), p.24
13. S.Mohren, PhD thesis, University of Heidelberg, 1996
14. M.A.Lisa et al., EOS collaboration, Phys. Rev. Lett. **75**, 2662 (1995)
15. J.P.Bondorf, A.S.Botvina, A.S.Iljinov, I.N.Mishustin and K.Sneppen, Phys. Rep. **257**, 133 (1995)
16. D.H.E.Gross, Rep. Progr. Phys. **53**, 605 (1990)
17. W.Reisdorf et al., FOPI collaboration, Nucl. Phys. A **612**, 493 (1997)
18. S.T.Butler and C.A.Person, Phys. Rev. **129**, 836 (1963)

19. V.D.Toneev and K.K.Gudima. Nucl.Phys. A **400**, 173c (1983)
20. L.P.Csernai and J.I.Kapusta, Phys. Rep. **131**, 223 (1986)
21. G.I.Kopylov, *Principles of resonance kinematics*, published by Nauka, (Moscow, 1970)
22. J.P.Bondorf et al., Phys. Rev. Lett. **73**, 628 (1994)
23. G.J.Kunde et al., Phys. Rev. Lett. **74**, 38 (1995)
24. W.Neubert et al., FOPI collaboration, in *Proceedings of the International Workshop on Heavy Ion Physics at Low, Intermediate and High Energies using 4 $\pi$  Detectors, Poiana Brasov, 1996* edited by M.Petrovici et al. (World Scientific, Singapore 1997) p.176
25. C.Williams et al., Phys. Rev. C **55**, R2132 (1997)
26. M.D'Agostino et al., Phys. Lett. B **371**, 175 (1996)
27. W.Reisdorf and H.G.Ritter, Annu. Rev. Part. Sci. **47**, 663 (1997)
28. M.A.Lisa et al. EOS Collaboration, in *Proceedings of the International Workshop on Heavy Ion Physics at Low, Intermediate and High Energies using 4 $\pi$  Detectors, Poiana Brasov, 1996* edited by M.Petrovici et al. ( World Scientific, Singapore 1997) p.194
29. K.G.R.Doss et al., Phys. Rev. C **37**, 16 (1988)
30. W.A.Friedman, Phys. Rev. C **42**, 667 (1990)
31. A.Ono, Phys. Rev. C **59** (1999) 853 and in *Summaries of the 7<sup>th</sup> International Conference on Clustering Aspects of Nuclear Structure and Dynamics, Rab, 1999*, edited by Z.Basrak et al., (Zagreb,1999) ,p. 89
32. A.Hombach et al., Eur. Phys. J. A **5**, 157 (1999)